



**HAL**  
open science

# Synthesis of Titanate Nanotubes Directly Coated with USPIO in Hydrothermal Conditions: A New Detectable Nanocarrier

Anne-Laure Papa, Lionel Maurizi, David Vandroux, Paul Walker, N. Millot

► **To cite this version:**

Anne-Laure Papa, Lionel Maurizi, David Vandroux, Paul Walker, N. Millot. Synthesis of Titanate Nanotubes Directly Coated with USPIO in Hydrothermal Conditions: A New Detectable Nanocarrier. *Journal of Physical Chemistry C*, 2011, 115 (39), pp.19012-19017. 10.1021/jp2056893 . hal-00785179

**HAL Id: hal-00785179**

**<https://hal.science/hal-00785179>**

Submitted on 11 Mar 2021

**HAL** is a multi-disciplinary open access archive for the deposit and dissemination of scientific research documents, whether they are published or not. The documents may come from teaching and research institutions in France or abroad, or from public or private research centers.

L'archive ouverte pluridisciplinaire **HAL**, est destinée au dépôt et à la diffusion de documents scientifiques de niveau recherche, publiés ou non, émanant des établissements d'enseignement et de recherche français ou étrangers, des laboratoires publics ou privés.

# Synthesis of titanate nanotubes directly coated with USPIO in hydrothermal conditions: a new detectable nanocarrier

*Anne-Laure Papa<sup>1#</sup>, Lionel Maurizi<sup>1#</sup>, David Vandroux<sup>2</sup>, Paul Walker<sup>3</sup> and Nadine Millot<sup>1\*</sup>*

<sup>1</sup> Laboratoire Interdisciplinaire Carnot de Bourgogne, UMR 5209 CNRS/Université de Bourgogne, 9  
avenue Alain Savary, BP 47870, 21078 Dijon cedex, France.

<sup>2</sup> NVH Medicinal, 57 rue Vannerie, 21000 Dijon, France.

<sup>3</sup> Département de Spectroscopie par Résonance Magnétique, Centre Hospitalier Universitaire de Dijon,  
2 Boulevard Maréchal de Lattre de Tassigny, 21033 Dijon, France.

# These authors contributed equally to this work.

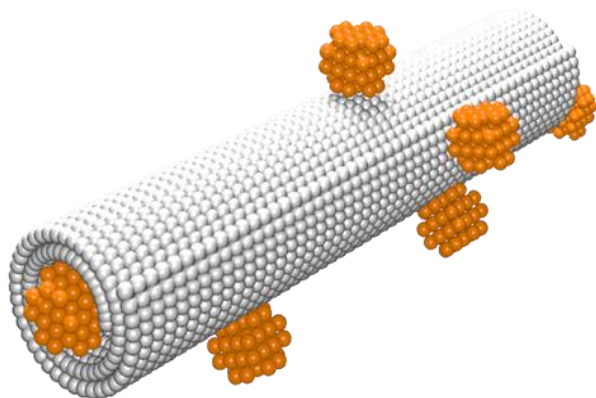
AUTHOR EMAIL ADDRESS: nmillot@u-bourgogne.fr

**RECEIVED DATE (to be automatically inserted after your manuscript is accepted if required  
according to the journal that you are submitting your paper to)**

CORRESPONDING AUTHOR FOOTNOTE \* Tel: +33 380 395 937 Email: nmillot@u-bourgogne.fr

ABSTRACT. For the first time, titanate nanotubes (TiONts) coated with USPIO (Ultrasmall Superparamagnetic Iron Oxide) without polymer functionalization and directly obtained during TiONts formation is reported. The coating of these tubes was performed directly during the TiONts hydrothermal synthesis. After this treatment, in strongly basic conditions, USPIO particles kept their structure and magnetic properties while their size distribution slightly increased. By coupling zeta potential measurements and TEM observations at different pH, it appeared that interactions between nanotubes and USPIO were not electrostatic. This study presents the new designing of a titanate needle shape nanocomposite capable of being detected by MRI for future biomedical applications.

TOC Graphic:



SECTION

Nanoparticles and nanostructures

KEYWORDS

Titanate nanotubes (TiONts), Ultrasmall SuperParamagnetic Iron Oxide (USPIO), hydrothermal synthesis, MRI detection, nanocarrier.

Titanate nanotubes (TiONts) have increasingly gained attention since their discovery<sup>1</sup>. They are generally synthesised by a hydrothermal treatment of a TiO<sub>2</sub> precursor (150 °C, 5 bar) in strongly basic conditions (NaOH, 10 mol.L<sup>-1</sup>)<sup>2</sup>. These nanotubes have a tubular morphology being rolled up in a spiral fashion, with an inner cavity: their length can attain several hundred nanometers and their diameter only a few nanometers ( $3\text{-}4\text{ nm} < d_{\text{inner}} < 10\text{ nm}$  and  $10\text{ nm} < d_{\text{outside}} < 20\text{ nm}$ )<sup>2</sup>. They also develop large specific surfaces depending on reaction parameters. These particularities induce an increase in the possible interactions with their outside environment.

Nanomedicines have attracted more and more attention over the last decade. Notably, this is reflected in the development of new therapeutics to target, detect and treat pathologies. Titanium oxides have revealed themselves as being promising material for biomedical applications. Indeed, titanium oxide surfaces have already been used as implantable devices<sup>3</sup>, pointing out the biocompatibility of titanium due to the TiO<sub>2</sub> passivation layer spontaneously formed on its surface. Recently, a study evaluated the effective stability of titanium dioxide (TiO<sub>2</sub>)-blasted dental implants over a 3-year period<sup>4</sup>. As for titanate nanotubes (TiONts), they have been used to replace hydroxyapatite in bone regeneration because they promote faster development of osteoblasts<sup>5</sup>. They have also been used as electrochemical biosensors for dopamine detection<sup>6</sup> in the diagnosis of Parkinson's disease.

To our knowledge, titanate nanotubes have not yet been reported in the literature for vectorisation studies in the biomedical field. Nonetheless, reports have already shown that the shape of nanoparticles, used as carriers, affects biodistribution<sup>7</sup>. It has also been shown previously that elongated shape organic nanoparticles were more easily internalised into cells than their spherical counterparts with similar volumes<sup>8</sup>. The needle shape of these nanotubes, leading to a high internalisation potential, was the rationale for future studies, with the prospect to evaluate the biodistribution of this new nanocarrier. Several possibilities may allow the detection of titanate nanotubes by imaging modalities: grafting a paramagnetic compound for Magnetic Resonance Imaging (MRI), grafting of radioisotopes

for Positron Emission Tomography (PET) or Single Photon Emission Computed Tomography (SPECT) and grafting of fluorescent dyes. The present paper reports the synthesis, the designing and the characterisation of a new TiONts-USPIO carrier for future studies of drugs vectorisation and MRI detection applications.

Today, nanotubes attract attention in the biomedical field. For example, Calucci *et al.* published in 2010 a study on boron nitride nanotubes as T<sub>2</sub>-weighted MRI contrast agents<sup>9</sup>. Additionally, carbon nanotubes (CNTs), have already been tested to deliver therapeutic or detection molecules<sup>10, 11</sup>. However, they have several major drawbacks: they are insoluble in most solvents<sup>12</sup> and their extremities are closed. In addition, they need to be functionalised to render them more hydrophilic. Several groups reported CNTs used as MRI contrast agents<sup>13</sup>. However, the attribution of susceptibility effects remains controversial. They were due to iron impurities for some<sup>12</sup>, and due to both the iron impurity and the CNTs themselves for others<sup>13</sup>. Notice that in most cases, studies published employed SWCNTs functionalized by Gd<sup>3+</sup> chelates<sup>14</sup> to obtain MRI contrast.

Different possibilities were encountered in the literature to obtain coated or doped TiONts. TiONts were typically coated with metal nanoparticles such as Au, Pd, Pt, RuO(OH), Ni and CdS which were used for catalysis<sup>15</sup>. Authors assumed that the metal nanoparticles were deposited on both internal and external surfaces of tubes. Previous studies have also described direct hydrothermal synthesis of titanate nanotubes doped with magnetic metal ions (Fe<sup>3+</sup>, Ni<sup>2+</sup>, Mn<sup>2+</sup>, Co<sup>2+</sup>)<sup>16, 17</sup>. Some authors have described iron oxide “tube-in-tube” nanostructures<sup>18, 19</sup>. After their hydrothermal synthesis, a thermal treatment allowed to convert hematite nanotubes into maghemite<sup>20</sup>. Another study described TiO<sub>2</sub> nanotubes functionalised by iron oxide nanoparticles<sup>21</sup>. These tubes were first synthesised by electrochemical anodisation (aligned tubes with much higher dimensions than those obtained by hydrothermal treatment: diameter about 100 nm) and they were then functionalised with iron nanoparticles by dextrin linking. A study deals with iron-coated TiO<sub>2</sub> nanotubes and is dedicated to photocatalytic studies<sup>22</sup>. The coating is obtained in two step: after titanate nanotubes synthesis by treatment with a Fe(OH)<sub>3</sub> solution. To the best of our knowledge, there have been no prior studies on

TiONts coated with USPIO during the hydrothermal synthesis of nanotubes without polymer linkage between both oxide particles. This is reported for the first time in the present study.

After hydrothermal synthesis, the resulting light brown coloured product, and in particular whitish filaments (Figure 1a), was attracted by magnetization (Figure 1b). This observation leads to two conclusions: i) iron oxide nanoparticles kept their magnetic properties during the 24 hours of hydrothermal treatment, ii) titanates were also attracted and proved a link between nanotubes and magnetic nanoparticles.

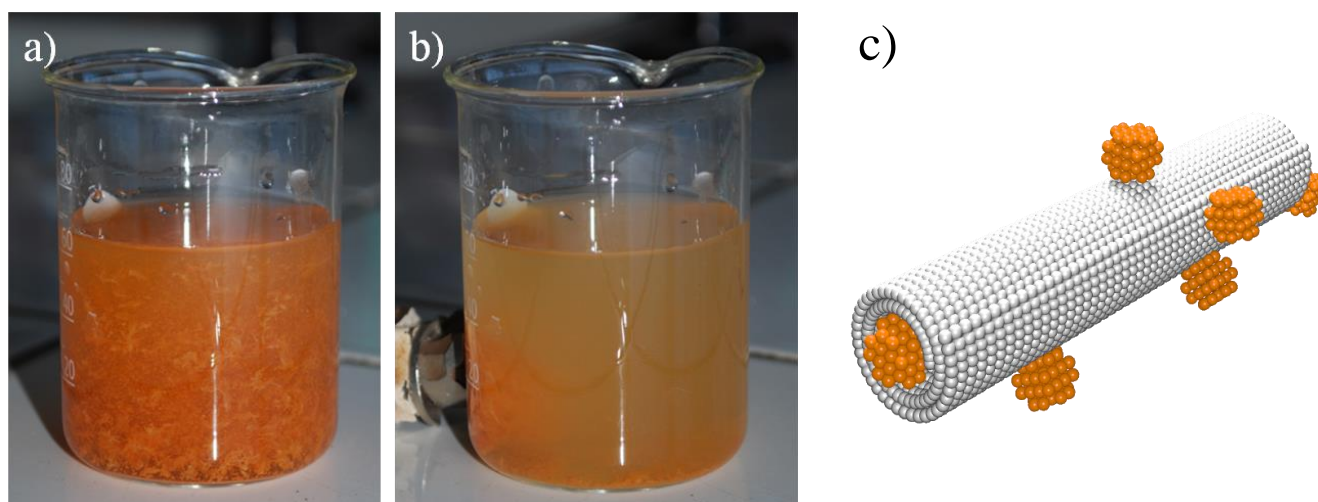


**Figure 1.** Product of TiONts synthesis in presence of USPIO just after the hydrothermal treatment in NaOH 10 mol.L<sup>-1</sup> and before dialysis: a) without and b) in the presence of a magnetic field. c) Representation of TiONts coated with USPIO.

TEM observations have shown that titanates had tubular morphology (Figure 2) as expected and described for the previously reported synthesis of TiONts<sup>2</sup>. The presence of iron oxide nanoparticles did not disturb a lot the "rolling up" mechanism of nanotubes and no other by-products such as remaining TiO<sub>2</sub> particles, titanate nanoribbons or nanosheets were observed. The only difference observed was a diameter distribution of TiONts when USPIO were added during nanotubes synthesis: between 10 nm (Figure 2 a1) and 20 nm (Figure 2 a2) in comparison with mostly 10 nm for the reference synthesis of TiONts (without USPIO)<sup>2</sup> (Figure 2d). A first explanation could be the inclusion

of USPIO particles into the TiONts inner cavity during the sheet rolling-up mechanism<sup>23</sup> and leading maybe to highest diameters figure 2c and 2d. Moreover, heterogeneities of the diameter along a single tube have been observed (Figure 2 a2), such perturbations may be due to USPIO inclusion in the inner cavity of the tube. Nevertheless, it remains difficult to be fully affirmative about this USPIO entrapment only thanks HRTEM investigation. Another explanation could be the influence of USPIO in solution which may affect the surface tension of the titanate sheets and modify nanotube enrollment. Indeed, small changes in synthesis parameters of titanate nanotubes could lead to chemical counterparts having different shapes (as nanowires, nanoribbons)<sup>2</sup>. So it is not exclude that the introduction of USPIO during tubes synthesis could also disturb the driving forces leading to the own morphology of the tubes (number of layers, diameter, etc...), as here about the diameter variation of the tubes (Figure 2d). Moreover, it is well known that modifications of nanoparticles surface, here nanotubes surface, lead to modifications of surface energy and surface stress, both responsible for structural disturbance.<sup>24 n</sup>

Concerning USPIO distribution on nanotubes surface, all TiONts carried USPIO, but not in a homogeneous way. Some tubes were abundantly coated (Figure 2 a2) while others were associated with only a few USPIO (Figure 2 a1). A schematic representation of TiONts/USPIO assemblies is shown on Figure 1c. Regarding iron oxide nanoparticles now, the mean size of USPIO measured by counting at least a hundred crystallites on HRTEM images, increased from  $(9.0 \pm 2.0)$  nm before hydrothermal synthesis to  $(11.5 \pm 2.0)$  nm after. This increase was probably due to Ostwald ripening in the basic NaOH solution necessary for TiONts formation.

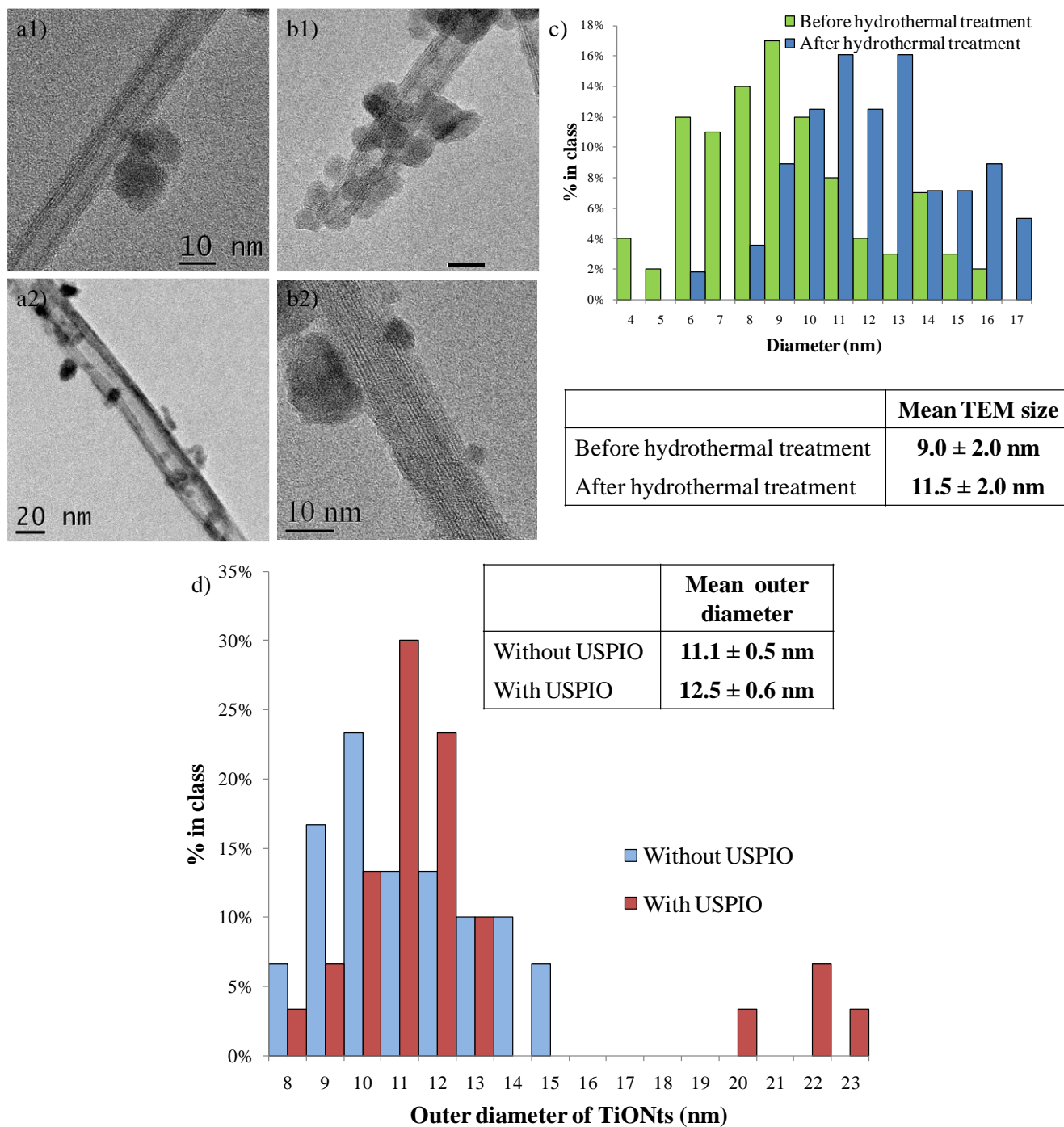


**Figure 2.** TEM images of TiONts coated with USPIO. These products were obtained (a1-a2) after hydrothermal treatment and washed to reach pH 5.5. b1-b2) from a previous suspension at pH 10 following NaOH addition. c) TEM size distribution of USPIO before and after hydrothermal treatment, d) outer diameter distribution of TiONts during their synthesis without or with USPIO.

Characteristic distances of both TiONts and spinel phase were identified by SAED (Selected Area Electron Diffraction) of the specimen (Figure 3). All the rings can be indexed as those belonging

to the two phases, and, no hematite formation was observed. Usually, the SAED pattern of TiONts presented another intense ring (halo rather than ring) corresponding to a d value of 0.76 nm corresponding to the interlayer distance between two consecutive tube walls. This distance was missing on this SAED pattern because it was hidden by the very close high intensity transmitted beam. On the other hand, all diffraction rings of maghemite were detectable except the low intensity ring of the (422) plane (expected at 0.17 nm with a relative intensity of 8.3% with respect to the most intense plane).

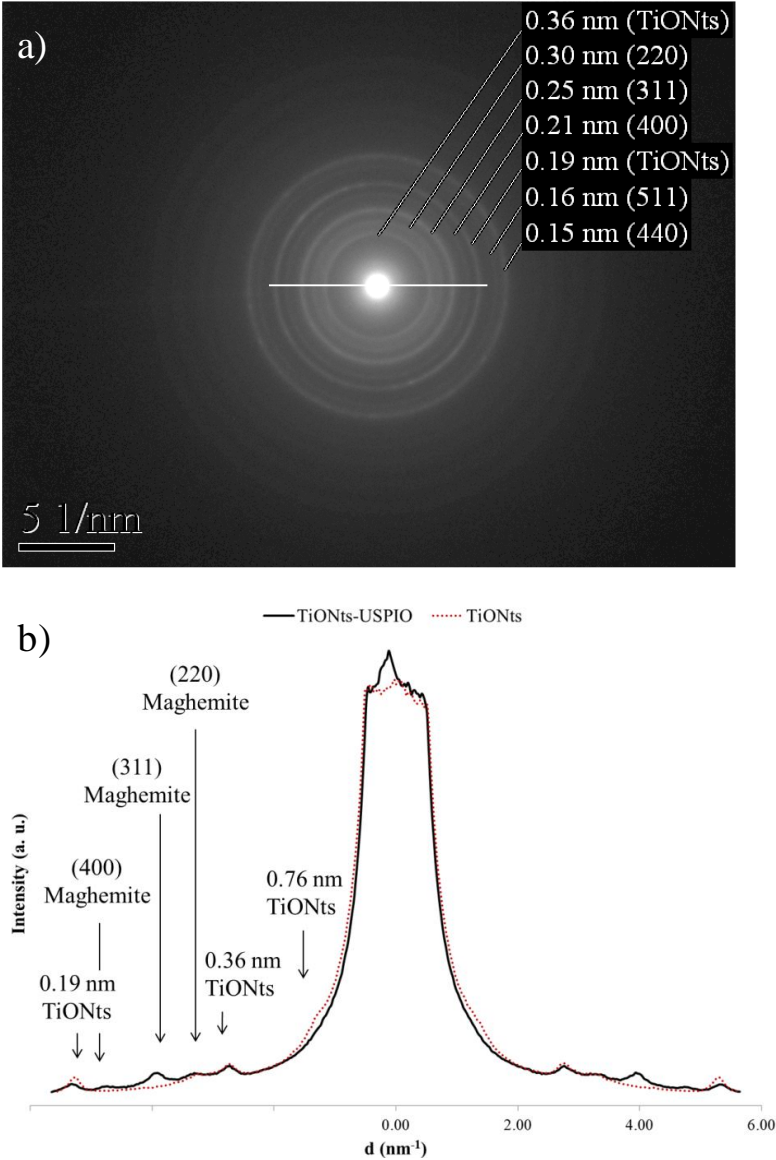


**Figure 3.** a) SAED (150 cm camera length) of TiONts coated with USPIO and b) SAED profiles along the white line on previous SAED. (hkl) reflections of maghemite (ICDD pattern 39-1346) were indexed.

Zeta potential curves of TiONts and USPIO had the same profile: zeta potential was positive below the isoelectric point (respectively 3.6 and 7.0) and negative above (Figure 4). Consequently, there was a pH domain (3.6 - 7.0) in which these two species can interact electrostatically. Hydrothermal synthesis of TiONts coated with USPIO was performed in NaOH (10 mol.L<sup>-1</sup>, pH 14). After synthesis, the resulting product was dialysed until pH 5.5 was reached. TEM observations of this product showed that USPIO were grafted on TiONts (Figure 2 a1-a2). To exclude the possibility of an electrostatic binding, the previous sample was brought to pH 10 by NaOH addition under magnetic stirring. TiONts and USPIO assemblies remained the same (Figure 2 b1-b2). Consequently, the link between both oxide surfaces appeared not to be electrostatic. Preliminary washings have been realized first by a centrifugation step (25 000 × g) followed by dialysis, both for uncoated nanotubes and for nanotubes/USPIO assemblies. Nanotubes formation is very sensitive to little variations in reaction parameters, in particular washing process, so first idea was to preserve the rolling-up mechanism leading to nanotubes by avoiding any change during washings.<sup>1, 2</sup> This methodology lead to the assemblies presented in this paper. It is noteworthy that USPIO and TiONts are not separated during both intensive centrifugation and long dialysis time, nor by application of a magnetic field (Figure 1b). Nevertheless, more intensive washings have been realized since, as centrifugation at various G (from 115 × g to 25 000 × g) alternate with ultrasounds but also ultrafiltration (with different membranes): in any case, the coating remains approximately the same.

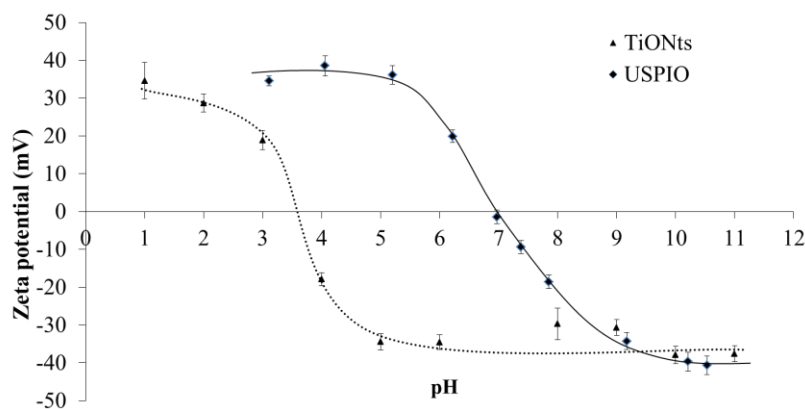


**Figure 4.** Zeta potential curves of TiONts (dotted line) and USPIO (black line) as a function of pH (in NaCl  $10^{-2}$  mol.L $^{-1}$ ). Isoelectric points of TiONts and USPIO were respectively about 3.6 and 7.0.

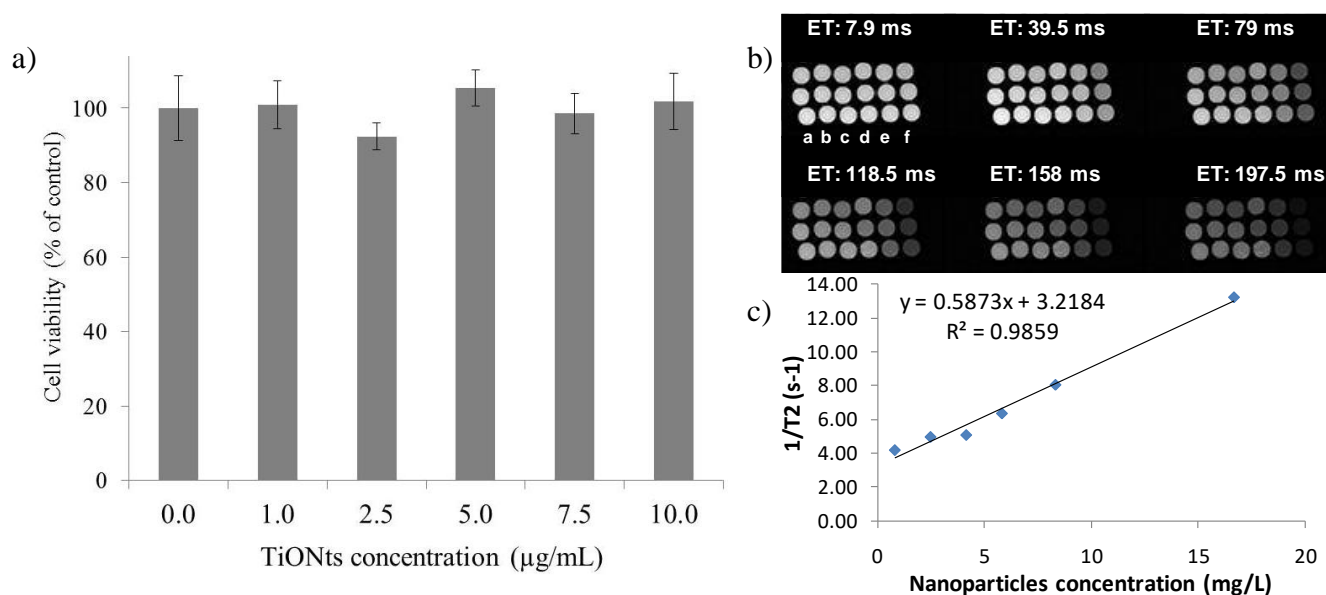


**Figure 5.** a) MTT assay of TiONts on CHO cells at 24h. Cell viability is expressed as the percentage of viable cells compared to the control. Error bars represent the standard deviation for four replicates; b) 3 Tesla MRI phantoms of TiONts labelled with USPIO at several concentrations (respectively from a to f: 0.8, 2.5, 4.2, 5.8, 8.3 and 16.7 mg<sub>nanoparticle</sub>.L $^{-1}$ ) which gave relaxation time T<sub>2</sub> for each concentration c) Curve of inverse of T<sub>2</sub> versus concentration where the gradient gives the r<sub>2</sub> relaxivity in mM<sub>Fe</sub> $^{-1}$ .s $^{-1}$ .

Finally, the cytotoxicity of these nanotubes was evaluated on CHO cells by MTT assay at 24 h. The results showed that no cytotoxicity was observed up to 10.0 μg/mL (Figure 5 a).

The magnetic properties of these TiONts/USPIO assemblies were tested *in vitro* on a clinical 3 Tesla MRI. These nano-objects developed a magnetic response as we first observed by application of a magnetic field (Figure 1b). Indeed, the magnetic efficiency (r<sub>2</sub> relaxivity) of this suspension, calculated with MRI phantoms (Figure 5 b-c), gave an average value around 0.59 L.mg<sub>nanoparticles</sub> $^{-1}$ .s $^{-1}$ , indicating the possibility to detect USPIO decorated TiONts by MRI (Figure 5 b). This value can be compared to the r<sub>2</sub> values of naked TiONts and USPIO which are respectively 0 and 2.35 L.mg<sub>nanoparticles</sub> $^{-1}$ .s $^{-1}$  and

prove that USPIO coupled with TiONts do not lose their superparamagnetic property. With this  $r_2$  MRI measurement it is possible to estimate the density of USPIO coating. Briefly, the relaxivity of TiONts-USPIO is only due to the iron oxide nanoparticles and if the value of  $r_2$  of this composite material ( $0.59 \text{ L.mg}_{\text{nanoparticles}}^{-1}.\text{s}^{-1}$ ) is compared to the  $r_2$  of the naked USPIO used in this study ( $2.35 \text{ L.mg}_{\text{nanoparticles}}^{-1}.\text{s}^{-1}$ ) the weight ratio of USPIO on nanotubes may be obtained, here 25 %. The mean diameter of those maghemite nanoparticles is 11.5 nm and the density 5.2 (ICDD pattern 39-1346). So the mass of a single  $\gamma\text{-Fe}_2\text{O}_3$  nanoparticle is  $4.14 \cdot 10^{-18} \text{ g}$  and 1 g of USPIO contains  $2.4 \cdot 10^{17}$  nanoparticles. Since for 1 g of USPIO there are 3 g of TiONts, thanks to the surface area of the naked TiONts ( $121 \text{ m}^2.\text{g}^{-1}$ ) we found a density of coating of  $6.7 \cdot 10^{-4} \text{ USPIO/nm}^2$  of TiONts. This value, linked to a weight ratio of 25 %, is much higher than the density of coating of the work of L. R. Hou *et al.* in the case of titanate coated by  $\text{SnO}_2$ <sup>24</sup> and far higher than the one obtain by An *et al.* with their method of iron coating on  $\text{TiO}_2$  nanotubes<sup>22</sup>. Our results are promising and are in any case sufficient to detect the nanotubes thanks to MRI.

For the first time, titanate nanotubes coating with USPIO are reported i) directly during hydrothermal synthesis of nanotubes and ii) without the use of an organic molecule linkage between both oxide particles. In comparison with a similar TiONts synthesis without USPIO, a distribution of nanotubes diameter was observed between 10 and 20 nm, which could be explained by the influence of USPIO on TiONts enrollment. TiONts coating was heterogeneous. After hydrothermal treatment in strongly basic conditions, iron oxide nanoparticles kept both their structure and their magnetic properties. A noteworthy increase of their mean crystallite size was nevertheless observed. By changing the pH and coupling with zeta potential and TEM observations, it appeared that interactions between nanotubes and USPIO were not electrostatic. Future studies will focus attention on the precise nature of these interactions (XPS and EXAFS experiments in progress). Moreover, these nanotubes have already been dispersed in water through different polymer graftings rendering the TiONts surface biocompatible.<sup>26</sup> This new design of titanate needle shape nanocomposites, detectable by MRI, opens

the door for future biodistribution studies of nanotubes to evaluate their potential as nanovectors and their toxicity.

## EXPERIMENTAL SECTION

*USPIO synthesis.* USPIO nanoparticles were prepared as described in the literature<sup>24, 27</sup>; the synthesis was optimized to obtain narrow grain size distribution. Briefly, a 1:2 molar ratio of ferrous and ferric chloride (respectively, 1 mol.L<sup>-1</sup> and 2 mol.L<sup>-1</sup>) was added drop by drop to a 0.75 mol.L<sup>-1</sup> NaOH solution at 90°C. After rinsing several times with HNO<sub>3</sub> (1 mol.L<sup>-1</sup>) and water, the final suspension was maintained at pH 3 with an USPIO concentration of 44 mg.mL<sup>-1</sup>.

*TiONts coated USPIO synthesis.* Titanate nanotubes were prepared by a classical hydrothermal method<sup>2</sup>. Fifty milligrams of titanium dioxide rutile precursor powder purchased from Tioxide were added to a NaOH aqueous solution (10 mol.L<sup>-1</sup>, 110 mL). The same amount of USPIO was mixed with the dioxide suspension (1/1, w/w) i.e. 1136 µL of the acidic suspension. pH of the suspension before hydrothermal treatment was 14. The mixture was submitted to ultrasound agitation (30 min, pulse 2 s, amplitude 50 %, 750 Watt, Sonics Vibra-Cells™) before being transferred to a sealed Teflon reactor under magnetic stirring (250 tr.min<sup>-1</sup>). The hydrothermal reactor temperature was kept at 150°C for 24 h. The resulting light brown colored product (Figure 1a) was isolated by centrifugation (25 000 × g during 10 min) and washed with deionized water by dialysis until a pH 5.5 was attained (it approximately takes 3 days). Finally, the suspension was freeze-dried.

*HRTEM Observations.* HRTEM observations were performed on a JEOL JEM-2100 LaB 6 microscope operating at 200 kV and equipped with a high tilt pole piece achieving a point-to-point resolution of 0.25 nm.

*Zeta potential measurements.* Zeta potentials were measured with a Malvern Nano ZS instrument supplied by DTS Nano V4.2 software.

*Cytotoxicity via MTT assay.* Cytotoxicity was evaluated by measuring the mitochondrial dependent reduction of 3-(4,5-dimethyliazol-2-yl)2,5-diphenyltetrazolium bromide (MTT, Sigma) to

formazan. Firstly, Chinese hamster ovary (CHO) cells (CHO-K1 cell line; ECACC) were cultured in DMEM media supplemented with 10% Fetal Bovine Serum before being stimulated in serum-deprived media when they reached 70% confluency. After 24 h of treatment, the cells were washed twice with PBS (NaCl 140 mM.L<sup>-1</sup>, KCl 2.7 mM.L<sup>-1</sup>, Na<sub>2</sub>HPO<sub>4</sub> 8.1 mM.L<sup>-1</sup>, and KH<sub>2</sub>PO<sub>4</sub> 1.5 mM.L<sup>-1</sup>) and incubated with MTT (2 mL, 2 mg.mL<sup>-1</sup> in Hanks medium) for 60 min at 37°C. Cells were then lysed by addition of the same volume of propane-2-ol and 0.1 mM.L<sup>-1</sup> HCl. The amount of formazan produced was detected by measurement of the absorbance at 570 nm with a spectrophotometer (VICTOR X3 apparatus, Perkin-Elmer).

*Relaxation time measurements.* Water proton transverse (T<sub>2</sub>) relaxation time measurements at 3.0 T were carried out at 298±1 K with a Siemens Magnetom Trio TIM using a commercially available birdcage head coil. Relaxation time measurements were performed on test tubes containing TiONts labelled with USPIO at different concentrations. For T<sub>2</sub> determination, a multi-echo spin-echo (SE) pulse sequence was used, with TR = 5000 ms, matrix = 256x204, FOV = 100x80 mm and slice thickness = 5 mm. Images were acquired at 32 echoes, starting at TE = 7.9 ms with a 7.9 ms interval. Image analysis was performed using ImageJ (Image Analysis Software developed by NIH, USA). The signal decay curve was fitted using a non-linear function to the equation  $S(TE) = A \exp(-TE/T_2)$ . The relaxivity, r<sub>2</sub>, was then determined by fitting the relaxation rate (1/T<sub>2</sub>) nanoparticles concentration in mg.L<sup>-1</sup>.

## ACKNOWLEDGMENTS

This work was supported by the Conseil Régional de Bourgogne. We would like to thank Dr. R. Chassagnon for HRTEM images, J. Paris for his help during syntheses and Dr. Laure Dumont for the cytotoxicity tests.

## REFERENCES

1. Kasuga, T.; Hiramatsu, M.; Hoson, A.; Sekino T.; Niihara, K. Titania nanotubes prepared by chemical processing. *Advanced Materials*. 1999, *11*, 1307-1311.
2. Papa, A. L.; Millot, N.; Saviot, L.; Chassagnon, R.; Heintz, O. Effect of reaction parameters on composition and morphology of titanate nanomaterials. *J. Phys. Chem. C*, 2009, *113*, 12682-12689.
3. Rupp, F.; Scheideler, L.; Olshanska, N.; de Wild, M.; Wieland, M.; Geis-Gerstorfer, J.; Enhancing surface free energy and hydrophilicity through chemical modification of microstructured titanium implant surfaces. *J. Biomed. Mater. Res. Part A*, 2006, *76A*, 323-334.
4. Veltri, M.; Ferrari M.; Balleri, P. Stability values of titanium dioxide-blasted dental implants in edentulous maxillas: a 3-year pilot study. *J. Oral Rehabil.*, 2010, *37*, 63-68.
5. Kubota, S.; Johkura, K.; Asanuma, K.; Okouchi, Y.; Ogiwara, N.; Sasaki, K.; Kasuga, T. Titanium oxide nanotubes for bone regeneration. *Journal of Materials Science-Materials in Medicine*, 2004, *15*, 1031-1035.
6. Niu, L. L.; Shao, M. W.; Wang, S.; Lu, L.; Gao, H. Z.; Wang, J. Titanate nanotubes: preparation, characterization, and application in the detection of dopamine. *Journal of Materials Science*, 2008, *43*, 1510-1514.7.
7. Decuzzi, P.; Godin, B.; Tanaka, T.; Lee, S. Y.; Chiappini, C.; Liu, X.; Ferrari, M. Size and shape effects in the biodistribution of intravascularly injected particles. *Journal of Controlled Release*, 2010, *141*, 320-327.
8. Gratton, S. E. A.; Ropp, P. A.; Pohlhaus, P. D.; Luft, J. C.; Madden, V. J. Napier M. E.; DeSimone, J. M. The effect of particle design on cellular internalization pathways. *Proceedings of the National Academy of Sciences of the United States of America*, 2008, *105*, 11613-11618.

9. Calucci, L.; Ciofani, G.; De Marchi, D.; Forte, C.; Menciassi, A.; Menichetti, L.; Positano, V. Boron Nitride Nanotubes as T<sub>2</sub>-Weighted MRI Contrast Agents. *Journal of Physical Chemistry Letters*, 2010, *1*, 2561-2565.10.
10. McDevitt, M. R.; Chattopadhyay, D.; Kappel, B. J.; Jaggi, J. S.; Schiffman, S. R.; Antczak, C.; Njardarson, J. T.; Brentjens, R.; Scheinberg, D. A. Tumor targeting with antibody-functionalized, radiolabeled carbon nanotubes. *J. Nucl. Med.*, 2007, *48*, 1180-1189.
11. Pantarotto, D.; Briand, J. P.; Prato, M.; Bianco, A. Translocation of bioactive peptides across cell membranes by carbon nanotubes. *Chem. Commun.*, 2004, 16-17.
12. Vaisman, L.; Wagner, H. D.; Marom, G.; The role of surfactants in dispersion of carbon nanotubes. *Advances in Colloid and Interface Science*, 2006, *128*, 37-46.
13. Al Faraj, A.; Cieslar, K.; Lacroix, G.; Gaillard, S.; Canot-Soulas, E. Cremillieux, Y. In Vivo Imaging of Carbon Nanotube Biodistribution Using Magnetic Resonance Imaging. *Nano Lett.*, 2009, *9*, 1023-1027.
14. Hartman, K. B.; Laus, S.; Bolskar, R. D.; Muthupillai, R.; Helm, L.; Toth, E.; Merbach A. E.; Wilson, L. J. Gadonanotubes as ultrasensitive pH-smart probes for magnetic resonance imaging. *Nano Lett.*, 2008, *8*, 415-419.
15. Bavykin, D. V.; Walsh, F. C.; Elongated Titanate Nanostructures and Their Applications. *Eur. J. Inorg. Chem.*, 2009, 977-997.
16. Wang, M. L.; Song, G. B.; Li, J.; Miao, L. D.; Zhang, B. H.; Direct hydrothermal synthesis and magnetic property of titanate nanotubes doped magnetic metal ions. *Journal of University of Science and Technology Beijing*, 2008, *15*, 644-648.
17. Bavykin, D. V.; Walsh, F. C.; Elongated Titanate Nanostructures and Their Applications. RSC Nanoscience & Nanotechnology No.12, 2010, ISBN: 978-1-84755-910-4.

18. Song, L. M.; Zhang, S. J.; Chen, B.; Ge, J. J.; Jia, X. C.; A hydrothermal method for preparation of  $\alpha$ -Fe<sub>2</sub>O<sub>3</sub> nanotubes and their catalytic performance for thermal decomposition of ammonium perchlorate. *Colloids Surf. Physicochem. Eng. Aspects*, 2010, 360, 1-5.
19. Suber, L.; Imperatori, P.; Ausanio, G.; Fabbri, F.; Hofmeister, H.; Synthesis, morphology, and magnetic characterization of iron oxide nanowires and nanotubes. *J. Phys. Chem. B*, 2005, 109, 7103-7109.
20. Jia, C. J.; Sun, L. D.; Yan, Z. G.; You, L. P.; Luo, F.; Han, X. D.; Pang, Y. C.; Zhang, Z.; Yan, C. H. Single-Crystalline Iron Oxide Nanotubes. *Angewandte Chemie-International Edition*, 2005, 44, 4328-4333.
21. Kontos, A. I.; Likodimos, V.; Stergiopoulos, T.; Tsoukleris, D. S.; Falaras, P.; Rabias, I.; Papavassiliou, G.; Kim, D.; Kunze, J.; Schmuki, P. Self-Organized Anodic TiO<sub>2</sub> Nanotube Arrays Functionalized by Iron Oxide Nanoparticles. *Chem. Mater.*, 2009, 21, 662-672.
22. An, H.; Li, J.; Zhou, J.; Li, K.; Zhu, B.; Huang, W. Iron-coated TiO<sub>2</sub> nanotubes and their photocatalytic performance. *Journal of Materials Chemistry*, 2010, 20, 603-610.
23. Zhang, S.; Peng, L.-M.; Chen, Q.; Du, G. H.; Dawson, G.; Zhou, W. Z. Formation Mechanism of H<sub>2</sub>Ti<sub>3</sub>O<sub>7</sub> Nanotubes. *Phys. Rev. Lett*, 2003, 91, 256103.
24. Belin, T.; Millot, N.; Villieras, F.; Bertrand, O.; Bellat, J. P. Structural variations as a function of surface adsorption in nanostructured particles. *J. Phys. Chem. B*, 2004, 108, 5333-5340.
25. Hou, L.-R.; Yuan, C.-Z.; Peng, Y. Synthesis and photocatalytic property of SnO<sub>2</sub>/TiO<sub>2</sub> nanotubes composites. *Journal of Hazardous Materials*, 2007, 139(2), 310-315.
26. Millot, N.; Papa, A. L.; Bellat, V.; Boudon, J.; Bisht, H. Dispersion of titanates nanotubes: comparison of PEI and PEG nanohybrids. To be submitted to *J. Phys. Chem. B* in 2011.

27. Maurizi, L.; Bisht, H.; Bouyer, F.; Millot, N. Easy Route to Functionalize Iron Oxide Nanoparticles *via* Long-Term Stable Thiol Groups. *Langmuir*, 2009, 25, 8857-8859.